Two-dimensionally relocatable microfiber-coupled photonic crystal resonator

Ju-Young Kim,[1,*] Myung-Ki Kim,[1] Min-Kyo Seo,[1] Soon-Hong Kwon,[3] Jong-Hwa Shin,[1] and Yong-Hee Lee[1,2]

[1]*Department of Physics, KAIST, Daejeon 305-701, Korea*
[2]*Department of Nanoscience and Technology (WCU), KAIST, Daejeon 305-701, Korea*
[3]*Nano Device Research Center, Korea Institute of Science and Technology, Seoul 136-791, Korea*
[*]*Corresponding author: juyoung@kaist.ac.kr*

Abstract: A photonic crystal microresonator is proposed in this study that is relocatable in two dimensions. A wavelength-scale resonator with high Q-factor (26,000) and high collection efficiency (80%) is formed and repositioned by simply placing and relocating a curved-microfiber to a new position on the surface of a two-dimensional square lattice photonic crystal slab. The formation of the resonator was confirmed by observing lasing of resonators. Infrared microscope images showed that the lasing site is two-dimensionally relocated *in-situ*. Spectral tuning was demonstrated by modifying the curvature of the microfiber. Functionalities, such as the two-dimensional relocation, spectral tuning and efficient extraction, which the curved-microfiber coupling offers, may provide an alternative way of coupling with a single quantum dot.

OCIS codes: (230.5298) Photonic crystals; (140.3945) Microcavities; (220.4241) Nanostructure fabrication; (140.5960) Semiconductor lasers.

References and links

1. O. Painter, R. K. Lee, A. Scherer, A. Yariv, J. D. O'Brien, P. D. Dapkus, and I. Kim, "Two-dimensional photonic band-gap defect mode laser," Science **284**, 1819-1821 (1999).
2. H.-G. Park, S.-H. Kim, S.-H. Kwon, Y.-G. Ju, J.-K. Yang, J.-H. Baek, S.-B. Kim, and Y.-H. Lee, "Electrically Driven Single-Cell Photonic Crystal Laser," Science **305**, 1444-1447 (2004).
3. K. Nozaki, T. Ide, J. Hashimoto, W. H. Zheng and T. Baba, "Photonic crystal point shift nanolaser with ultimate small modal volume," Electron. Lett. **41**, 843-845 (2005).
4. T. Tanabe, M. Notomi, S. Mitsugi, A. Shinya, and E. Kuramochi, "All-optical switches on a silicon chip realized using photonic crystal nanocavities," Appl. Phys. Lett. **87**, 151112 (2005).
5. M.-K. Kim, I.-K. Hwang, S.-H. Kim, H.-J. Chang, and Y.-H. Lee, "All-optical bistable switching in curved microfiber-coupled photonic crystal resonators," Appl. Phys. Lett. **90**,161118 (2007).
6. T. Yoshie, A. Scherer, J. Hendrickson, G. Khitrova, H. M. Gibbs, G. Rupper, C. Ell, O. B. Shchekin, and D. G. Deppe, "Vacuum Rabi splitting with a single quantum dot in a photonic crystal nanocavity," Nature **432**, 200-203 (2004).
7. K. Hennessy, A. Badolato, M. Winger, D. Gerace, M. Atatüre, S. Gulde, S. Fält, E. L. Hu, and A. Imamoğlu, "Quantum nature of a strongly coupled single quantum dot-cavity system," Nature **445**, 896-899 (2007)
8. D. Englund, A. Faraon, I. Fushman, N. Stoltz, P. Petroff and J. Vučković, "Controlling cavity reflectivity with a single quantum dot," Nature **450**, 857-861 (2007)
9. B. S. Song, S. Noda, T. Asano, and Y. Akahane, "Ultra-high-Q photonic double-heterostructure nanocavity," Nat. Mater. **4**, 207-210 (2005).
10. T. Tanabe, M. Notomi, E. Kuramochi, A. Shinya and H. Taniyama, "Trapping and delaying photons for one nanosecond in an ultrasmall high-*Q* photonic-crystal nanocavity," Nat. Photonics **1**, 49-52 (2006)
11. S.-H. Kwon, T. Sünner, M. Kamp, and A. Forchel, "Ultrahigh-Q photonic crystal cavity created by modulating air hole radius of a waveguide," Opt. Express **16**, 4605-4614 (2008)
12. B.-S. Song, T. Asano and S. Noda, "Physical origin of the small modal volume of ultra-high-Q photonic double-heterostructure nanocavities," New J. Phys. **8** 209 (2006)
13. S. Tomljenovic-Hanic, C. M. Sterke, and M. J. Steel, "Design of high-Q cavities in photonic crystal slab heterostructures by air-holes infiltration," Opt. Express **14**, 12451-12456 (2006)

#110883 - $15.00 USD Received 4 May 2009; revised 8 Jul 2009; accepted 8 Jul 2009; published 15 Jul 2009

14. C. L. C. Smith, D. K. C. Wu, M. W. Lee, C. Monat, S. Tomljenovic-Hanic, C. Grillet, B. J. Eggleton, D. Freeman, Y. Ruan, S. Madden, B. Luther-Davies, H. Giessen, and Y.-H. Lee, "Microfluidic photonic crystal double heterostructures," Appl. Phys. Lett. **91**, 121103 (2007).
15. S. Gardin, F. Bordas, X. Letartre, C. Seassal, A. Rahmani, R. Bozio, and P. Viktorovitch, "Microlasers based on effective index confined slow light modes in photonic crystal waveguides," Opt. Express **16**, 6331-6339 (2008)
16. M.-K. Seo, J.-H. Kang, M.-K. Kim, B.-H. Ahn, J.-Y. Kim, K.-Y. Jeong, H.-G Park, and Y.-H. Lee, "Wavelength-scale photonic-crystal laser formed by electron-beam-induced nano-block deposition," Opt. Express **17**, 6790-6798 (2009).
17. S. Tomljenovic-Hanic, M. J. Steel, C. M. Sterke, and D. J. Moss, "High-Q cavities in photosensitive photonic crystals," Opt. Lett. **32**, 542-544 (2007)
18. M. Notomi and H. Taniyama, "On-demand ultrahigh-Q cavity formation and photon pinning via dynamic waveguide tuning," Opt. Express **16**, 18657-18666 (2008)
19. M.-K. Kim, I.-K. Hwang, M.-K. Seo, and Y.-H. Lee, "Reconfigurable microfiber-coupled photonic crystal resonator," Opt. Express **15**, 17241-17247 (2007).
20. C. Kim, W. J. Kim, A. Stapleton, J.-R. Cao, J. D. O'Brien, and P. D. Dapkus, "Quality factors in single-defect photonic-crystal lasers with asymmetric cladding layers," J. Opt. Soc. Am. B **19**, 1777-1781 (2002).
21. S. G. Johnson, S. Fan, P. R. Villeneuve, J. D. Joannopoulos, and L. A. Kolodziejaki, "Guided modes in photonic crystal slabs," Phys. Rev. B **60**, 5751–5758 (1999).
22. I.-K. Hwang, S.-K. Kim, J.-K. Yang, S.-H. Kim, S.-H. Lee, and Y.-H. Lee, "Curved-microfiber photon coupling for photonic crystal light emitter," Appl. Phys. Lett. **87**, 131107 (2005).
23. M. Meier, A. Mekis, A. Dodabalapur, A. Timko, R. E. Slusher, J. D. Joannopoulos and O. Nalamasu, "Laser action from two-dimensional distributed feedback in photonic crystals," Appl. Phys. Lett. **74**, 7-9 (1999).
24. S. Noda, M. Yokoyama, M. Imada, A. Chutinan and M. Mochizuki, "Polarization Mode Control of Two-Dimensional Photonic Crystal Laser by Unit Cell Structure Design," Science **293**, 1123-1125 (2001).
25. S.-H. Kwon, H.-Y. Ryu, G.-H. Kim, and Y.-H. Lee, "Photonic bandedge lasers in two-dimensional square-lattice photonic crystal slabs," Appl. Phys. Lett. **83,** 3870-3872 (2003).
26. K. Kiyota, T. Kise, N. Yokouchi, T. Ide, and T. Baba, "Various low group velocity effects in photonic crystal line defect waveguides and their demonstration by laser oscillation," Appl. Phys. Lett. **88**, 201904 (2006).
27. M. Notomi, K. Yamada, A. Shinya, J. Takahashi, C. Takahashi, and I. Yokohama, "Extremely large group velocity dispersion of line-defect waveguides in photonic crystal slabs," Phys. Rev. Lett. **87**, 253902 (2001).

1. Introduction

Photonic crystal (PC) resonators [1-11] have gained attention because of their ability to strongly confine photons within a small volume. Many applications, such as low-threshold lasers [1-3], all-optical switching [4, 5], on-chip cavity quantum electrodynamics (QED) experiments [6-8] are demonstrated based on high quality factor (Q), small mode volume (V) PC resonators. PC resonators of ultrahigh-Q over millions with mode volume of cubic wavelength have been proposed and realized [9-11].

Most of recent ultrahigh-Q PC resonator designs are based on PC waveguide structures which support slow light modes at the flat dispersion edge [9-11]. In these cases, strong light confinements can be achieved with slight local modification of the waveguide [12]. Resonators at a desired position can be easily made in the post-processing step. Various types of post-processed resonators are proposed and realized by infiltrating fluid [13, 14], coating polymer [15], depositing electron-beam-induced nano-blocks [16], and by changing refractive index [17, 18]. However, most of post-processing is irreversible [13-17] and difficult to apply *in-situ*.

A novel alternative, a curved-microfiber, was employed to create ultrahigh-Q resonators at desired positions [19]. Relocation of the resonator is possible by simple relocation of a curved-microfiber along a waveguide line. The relocation of resonators becomes particularly useful when the location of the photon emitter, such as a quantum dot (QD), is not known a priori. This provides continual opportunities to form a resonator until the resonator is created at the right place (e.g. QD sites). The relocation of the proposed resonator [19] is limited to one-dimension (1-D) because resonators are formed only above the pre-defined 1-D waveguide line.

#110883 - $15.00 USD Received 4 May 2009; revised 8 Jul 2009; accepted 8 Jul 2009; published 15 Jul 2009

In this paper, the dimension of the relocation is extended into two. The curved-microfiber can create the wavelength-scale PC resonator at a desired position even in the absence of the pre-defined waveguide structure. This method allows two-dimensional (2-D) relocations of the PC resonators because any points of the bare 2-D PC pattern can be chosen as the contact point of the curved-microfiber. The formation of the PC resonators is confirmed by experimentally observing laser operation of the resonators. The curved-microfiber directly collects the photons through evanescent coupling. Spectral resonance tuning was also demonstrated by adjusting the curvature of the curved-microfiber.

2. Concepts and computations

The 2-D scheme does not involve any PC waveguides unlike a previous report [19]. The straight-microfiber induces linear waveguide modes by increasing the effective index of the PC slab along the coupling direction. The cutoff frequency of waveguide modes are controlled by the air-gap distance between the microfiber and the PC slab. The curved-microfiber creates the 2-D relocatable resonator at the contact point on the PC slab. Light is trapped inside a Gaussian-shape photonic well, the spatial profile of the cutoff frequency constructed by the curved-microfiber. Discrete resonator modes are generated inside the photonic well.

Three-dimensional (3-D) finite-difference time-domain (FDTD) methods with periodic boundary conditions were used for calculating the dispersion and field patterns of the microfiber-induced waveguide modes. The same FDTD methods with perfectly matched boundary conditions were used for calculating Q-factor, mode-volume and field profiles of a relocatable resonator. Photon collection efficiency into the microfiber was calculated by the ratio of the integrated energy flux through the microfiber to the total outgoing flux through all calculation domain boundaries. The diameter of the microfiber was set at 1.0 μm where the step-index silica (n=1.45) cylinder operates as a single mode at a wavelength of 1.5 μm. The square lattice of air holes were defined on the 200-*nm*-thick slab (n=3.4) with a periodicity (a) of 500 *nm*. The radius (r) of the air holes was 0.35a. The photonic bandgap is formed for TE-like modes around ω_n=0.33, near 1.5 μm. A square lattice PC was chosen because it supports the fiber-induced resonant mode of Q value higher than that of the triangular lattice counterpart. The fiber-induced resonant mode tends to couple to TM-like propagation modes and becomes lossy [20], in the case of the triangular lattice.

2.1 Formation of waveguide modes

A straight-microfiber was placed on the square lattice PC slab along the Γ−X direction (Fig. 1(a)). The Γ−X direction is the nearest-neighbor direction of the square lattice. Linear waveguiding along other directions is less feasible because the folding of the light cone deteriorates the photonic band gap [21]. The microfiber increases the effective index of the PC slab by perturbing the evanescent tail of the bare PC extended modes and develops the PC waveguide modes beneath the microfiber. The dispersion characteristics of induced waveguide modes are shown in Fig. 1(b). New waveguide modes (red curve) were created inside the photonic bandgap, formed between the slab bands. The bands of the bare PC slab are depicted with gray regions. The E_y and H_z patterns of a waveguide-mode at the dispersion edge (k_n=0.5) are presented in the inset of Fig. 1(b) and Fig. 1(c), respectively. The fields are well confined inside the photonic crystal slab beneath the straight-microfiber. The dispersion edge of the induced waveguide modes is flat like the typical dispersion edge of PC waveguides. Between the dispersion edge (the cutoff) and the top of the first slab band, a 'mode-gap' is formed where light propagation is not allowed. The mode-gap confines the light with a frequency lower than the cutoff.

The cutoff frequency (frequency at k_n=0.5) strongly depends on the air-gap distance between the microfiber and the PC slab. It decreases as the microfiber comes closer to the PC slab due to the increased-effective-index of the PC slab (Fig. 1(d)). The cutoff frequency of the microfiber-induced waveguide falls off from ω_n=0.3348 and decreases down to the minimum, ω_n=0.3293, when the microfiber is in contact with the PC slab. The spectral

#110883 - $15.00 USD Received 4 May 2009; revised 8 Jul 2009; accepted 8 Jul 2009; published 15 Jul 2009

variance ($\Delta\omega$) between the cut-off frequencies with and without fiber was 0.0055, equivalent to $\Delta\lambda$=24.9 *nm* at a wavelength of 1.5 μm. The contact of the curved-microfiber constructs the spatial profile of the cutoff frequency depending on the air-gap distance. The waveguide modes at the contact point are confined due to its lowest cutoff frequency.

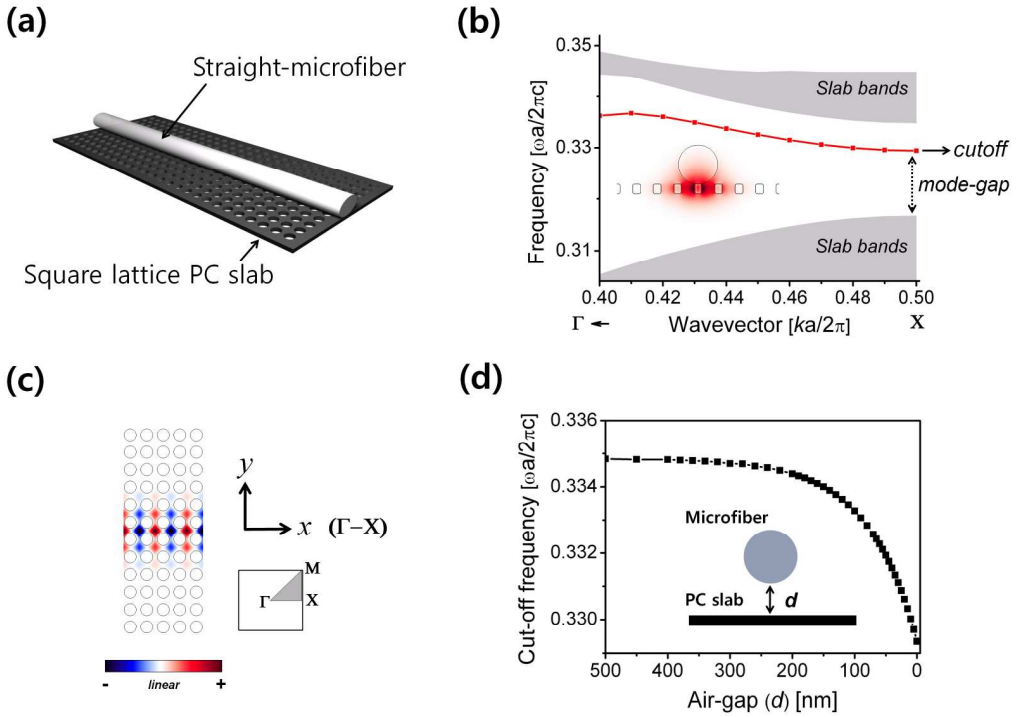

Fig. 1. The formation of waveguide modes in the square lattice photonic crystal slab. Straight-microfiber lies along the Γ–X line of the square lattice. (a) Illustration of the structure. (b) Dispersion of the microfiber-induced waveguide modes (red curve). The inset is the vertical cross section of the E_y pattern at X (k_n=0.5). (c) Horizontal cross section of the H_z pattern at X. The Brillouin zone of the square lattice is displayed at the right comer. (d) The cut-off frequencies of the waveguide modes as the microfiber approaches to the PC slab.

2.2 Formation of 2-D relocatable resonator

The air-gap distance between the microfiber and the PC slab varies quadratically when the curved-microfiber is in contact with 2-D PC slab. The cutoff frequency follows a Gaussian shape when plotted as a function of distance from the point of contact (dark yellow line in Fig. 2(c)). Photons with a specific frequency are confined inside the Gaussian photonic well. The first three resonator modes of the photonic well are found through the FDTD computations. The radius of the curvature (R) of the microfiber is R=70 μm. The E_y field profiles of the fundamental mode (0^{th}) and higher-order modes (1^{st} and 2^{nd}) are shown in the right side of the Fig. 2(c). The line graphs of the E_y pattern at the center (y=0) are overlapped with the profile of the cut-off frequency according to their resonant frequencies in order to visualize the confinement of the fields inside the Gaussian photonic well. Red, orange, and blue lines correspond to 0^{th}, 1^{st}, and 2^{nd} mode, respectively.

The fundamental mode (0^{th}) has a high Q-factor of 25900 and high collection efficiency into the microfiber of 80% (r=0.35a). Photons are confined in the proximity of the contact point and evanescently coupled to the microfiber (Fig. 2(b)). The mode volume is calculated to be 2.4x $(\lambda/n)^3$. The Q-factor of the fundamental mode is further increased up to 2.5x 10^5 if the collection efficiency is reduced to nearly zero by tuning the phase matching between the microfiber mode and the resonator mode. Phase matching is adjustable by changing the radius

#110883 - $15.00 USD Received 4 May 2009; revised 8 Jul 2009; accepted 8 Jul 2009; published 15 Jul 2009

of air-holes of the PC and off-coupling regime for ultrahigh-Q is obtained with r=0.31a. The higher-order modes have smaller Q-factors and larger mode-volumes than those of the fundamental mode. When r=0.35a, Q-factors of the 1st and 2nd modes were 3,880 and 1,480 and their mode volumes were 6.0x $(\lambda/n)^3$ and 9.9x $(\lambda/n)^3$, respectively.

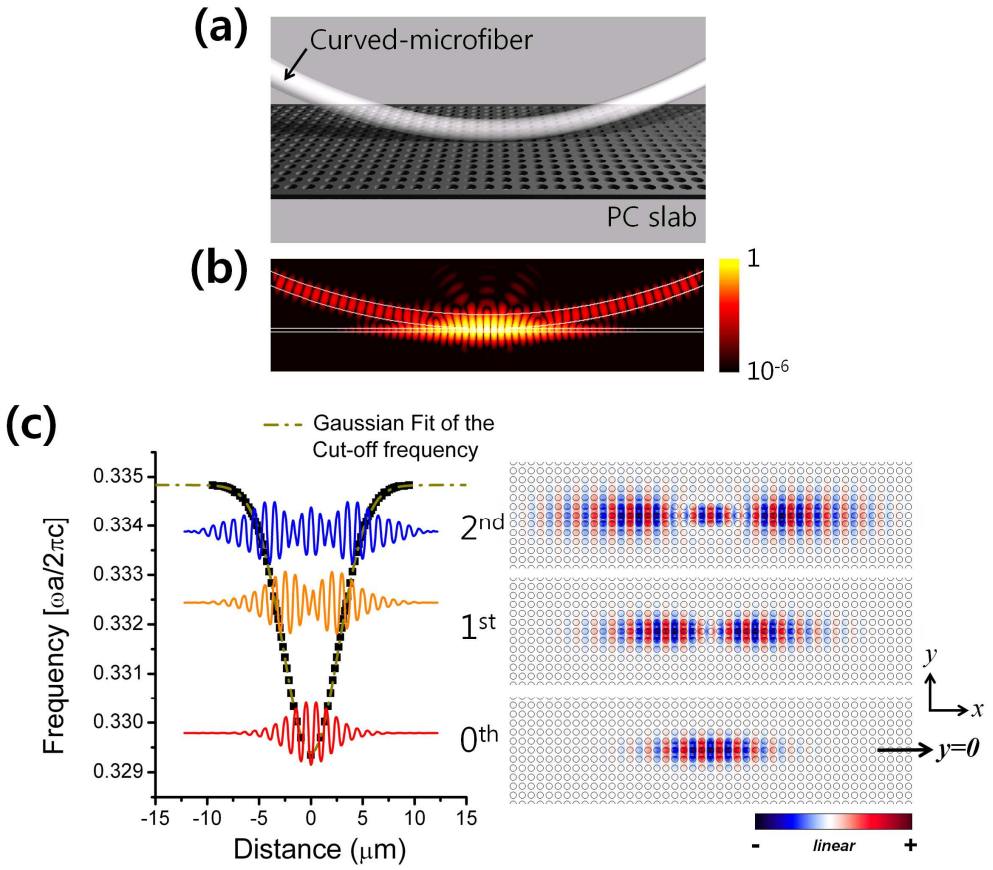

Fig. 2. (a) Scheme of the 2-D relocatable PC resonator (b) Electric field intensity of the fundamental mode (0th) (c) Spatial profile of the cut-off frequency (left) and the E_y patterns of the 2-D relocatable resonator modes at the slab center (right). Line graphs of the patterns at the fiber contact line (y=0) are overlapped with the profile of the cut-off frequency according to their resonant frequencies (left). Red, orange, and blue lines correspond to 0th, 1st, and 2nd mode, respectively.

3. Experiment

3.1 Sample preparation and experimental setup

Square lattice PC patterns were fabricated on a 200-*nm*-thick InGaAsP slab which contained four quantum wells in the middle as an active medium. The size of the pattern is 50 x 20 μm^2 which is large enough to provide a room for 2-D relocations (Fig. 3(a)). The inset of Fig. 3(a) shows a scanning electron microscopy (SEM) image of square lattice PC. The lattice constant (a) and the air hole radius (r) were 530 *nm* and 0.35a, respectively. A curved-microfiber is fabricated by tapering a single mode fiber down to 1.0 μm and bent such that R is ~90 μm (Fig. 3(b)). R of the microfiber is tuned larger or smaller than that of the fabricated one by pushing or pulling the microfiber toward or away from the slab once it makes contact with the PC slab. The control of the curvature changes the profile of the Gaussian photonic well and modifies

#110883 - $15.00 USD Received 4 May 2009; revised 8 Jul 2009; accepted 8 Jul 2009; published 15 Jul 2009

the characteristics of the resonator. The control of the curvature is exploited to tune the resonance wavelength of the 2-D relocatable resonator.

The sample was loaded on the rotating stage and rotated until the boundary of the pattern appears aligned with the microfiber in the CCD image. The boundary of the square pattern is in the Γ-X direction. The position of the curved-microfiber was adjusted by piezoelectric actuators with the precision of better than 30 nm.

A 980-nm pulsed pump laser light was sent through one end of the curved-microfiber. Quantum wells of the PC slab are pumped locally by the evanescent field of the pump laser guided by the curved-microfiber. Light from the resonator couples evanescently to the same curved-microfiber and is directly sent to the optical spectrum analyzer [22]. The width of the pumping pulse is 20 *ns* at the repetition rate of 1 MHz. Vertically-radiated emission into free space was collected by a 20X objective lens (N.A.=0.42) and captured by an infrared (IR) camera (Fig. 4(b)).

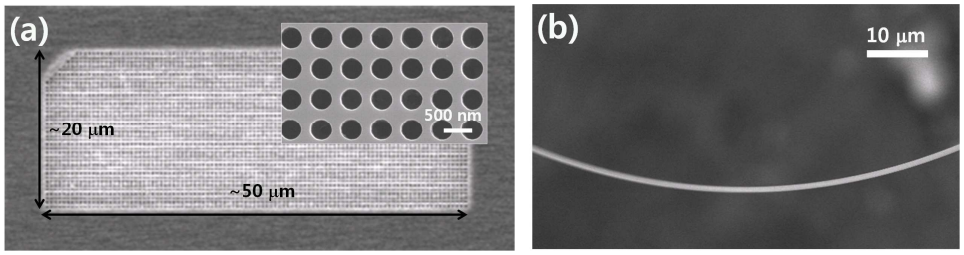

Fig. 3. SEM images of (a) the fabricated square lattice PC defined on the InGaAsP slab and (b) the fabricated curved-microfiber. The inset of (a) is the magnified image of the PC pattern.

3.2 Lasing spectra and 2-D relocations

Laser oscillation is observed near wavelength of 1.5 μm when the curved-microfiber is in contact with the PC slab and aligned along the Γ-X direction of the square lattice. A lasing spectrum is shown in Fig. 4(a). Strong laser emissions were recorded at a wavelength of 1505.5 *nm*. Two more peaks with weaker intensities follow at shorter wavelengths of 1493.8 and 1486.1 *nm*. The three peaks are the first three resonator modes formed in the Gaussian photonic well constructed by the curved-microfiber (Fig. 2(c)). The spectral separations ($\Delta\lambda$) between these three peaks agree well with those of FDTD computations. The measured first $\Delta\lambda_1$ (between 0^{th} and 1^{st} modes) and the second $\Delta\lambda_2$ (between 1^{st} and 2^{nd} modes) were $\Delta\lambda_1$=11.7 *nm* and $\Delta\lambda_2$=7.7 *nm*, respectively. Calculated values were $\Delta\lambda_1$=11.3 *nm* and $\Delta\lambda_2$=6.5 *nm*. The fundamental mode (0^{th}) lases first due to the highest Q-factor. The peak pump power at threshold was about 650 μW (Fig. 4(a)).

The relocatable resonator was repeatedly tested by detaching and relocating the curved-microfiber at arbitrary points in the two-dimensional PC pattern as long as the fiber is aligned along Γ-X direction. In comparison, when the fiber was aligned along Γ-M direction, no lasing was observed. The IR-camera images taken after moving the curved-microfiber to different locations is shown in Fig. 4(b). The dotted rectangle in Fig. 4(b)-1 indicates the boundary of the PC pattern. The black curve passing though the pattern is the curved-microfiber. White bright localized lasing spots were detected at various positions over the two-dimensional PC pattern. The lasing wavelengths, however, varied slightly because of the variation of the air hole size. The wavelengths of 0^{th} modes were 1527.9, 1519.0, 1505.5, and 1504.7 *nm* for patterns 1, 2, 3, and 4, respectively (Fig. 4(b)). FDTD computations predicted a 30 *nm* shift in wavelength for the radius change in air holes of 5 *nm*. The difference in *R*, when the curved-microfiber contacts on the slab, also affects the resonant wavelengths. The tuning of the resonant wavelength by adjusting *R* of the microfiber is discussed. The wavelength tuning of 8.4 *nm* was demonstrated using the control of the curvature.

#110883 - $15.00 USD Received 4 May 2009; revised 8 Jul 2009; accepted 8 Jul 2009; published 15 Jul 2009

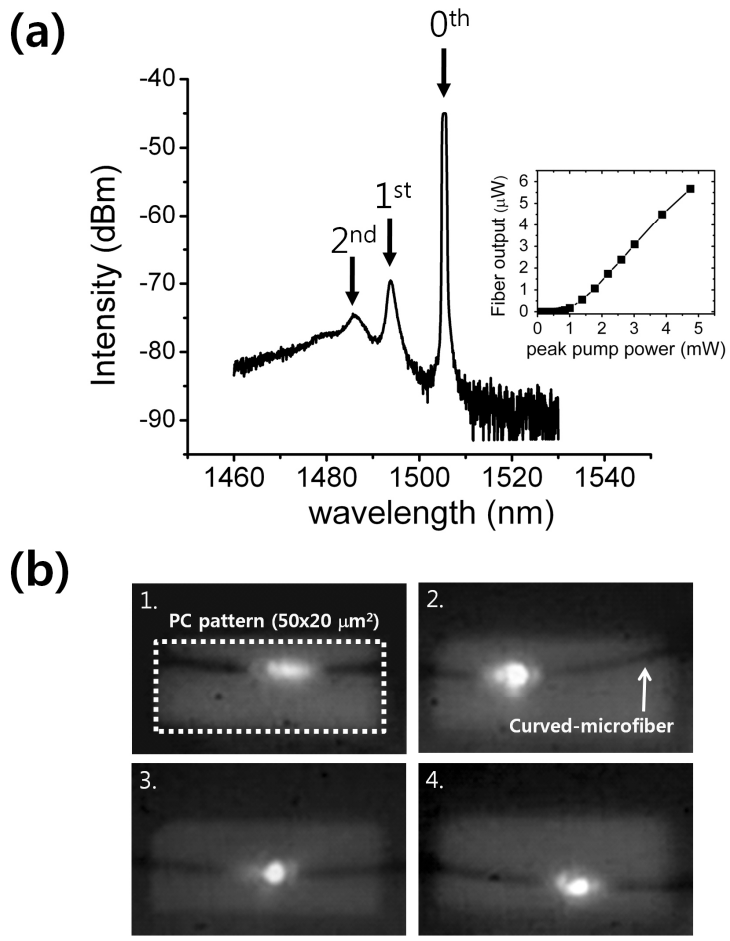

Fig. 4. (a) Lasing spectrum when the curved-microfiber contacts on the square lattice PC slab (the peak pump power is 2 *mW*). The L-L curve of the fundamental mode (0^{th}) is shown in the inset. (b) Relocations of the curved-microfiber coupled PC resonators. Localized laser emission spots are detected from various positions in the two-dimensional PC pattern where the microfiber contacts. The images are captured by an infrared camera.

The large separation between the lasing modes excludes the possibility of band edge lasing [23-25]. In the case of the band edge lasing, the spectral interval between the successive modes is estimated by the Fabry-Perot condition $\Delta k = \pi / L$, where L is the size of the photonic crystal pattern [26, 27]. When L is 50 μm, the spacing of the resonant wavevector (Δk) is 0.005, which corresponds to a wavelength separation of 0.18 *nm* at the upper edge of the bandgap. Typically, the in-plane band-edge mode scatters strongly at the boundaries of the pattern [25]. However, the measured emission spots are localized and placed beneath the contact points of the curved-microfiber in the middle of the pattern.

Efficient light extraction through the microfiber is provided and the extracted light is sent to optical systems without additional optics [22]. Over 5 μW peak output power was collected through one port of the curved-microfiber (Fig. 4(a)).

3.3 Spectral tunability

Spectral tuning of the resonator was achieved by adjusting the curvature of the curved-microfiber in addition to the 2-D spatial relocation. The length of resonator is increased effectively when R is increased. The increase in the length of the resonator results in the red-shift of the resonant wavelength. The curved-microfiber was pushed toward the PC slab until

#110883 - $15.00 USD Received 4 May 2009; revised 8 Jul 2009; accepted 8 Jul 2009; published 15 Jul 2009

contact. The fiber was moved backwards from the PC slab while maintains contact. This was the minimum *R* case. The lasing spectra were repeatedly measured by gradually increasing *R* from pushing the curved-microfiber down on the PC slab. The incident peak pump power was fixed at 5 *mW*. The lasing wavelength of the 0^{th} mode red-shifed by 8.4 *nm* from 1497.1 to 1505.5 *nm* as *R* increases (Fig. 5(a)). The process is reversible, allowing *in-situ* tuning of the resonator with real-time monitoring. The curvature-dependent spectral tuning is explained by 3-D FDTD analyses. The wavelength of the 0^{th} mode red-shifted by 7.5 *nm* when *R* is increased from 20 to 150 μm (Fig. 5(b)).

As *R* increases, the increase of the effective coupling length of the evanescent pump light may cause a slight rise of the temperature. Wavelength shift was measured as the pump power increases by fixing *R*, to observe the temperature effect solely. A 0.5 *nm* red-shift was observed when the pump power was increased from 1 *mW* to 5 *mW*. This is much smaller than the measured spectral shift.

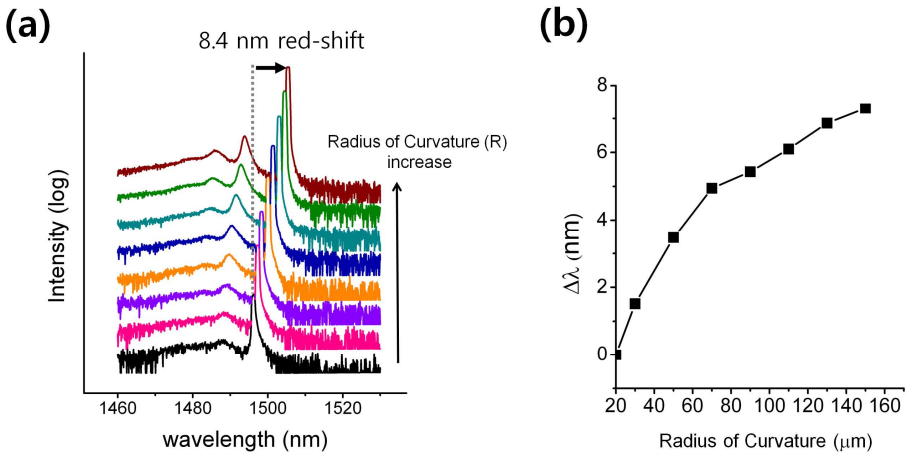

Fig. 5. (a) Spectral tuning of the 2-D relocatable resonator with increase of curvature (*R*) of the curved-microfiber. The lasing wavelength was red-shifted by 8.4 nm from 1497.1 nm to 1505.5 nm (b) Shift of the resonant wavelength of the fundamental mode (0^{th}) predicted by 3-D FDTD computations with increase in *R*.

4. Summary

A 2-D relocatable PC resonator was demonstrated by coupling a curved-microfiber to a square lattice PC slab. Wavelength-scale resonators are created in the proximity of the contact point of a curved-microfiber. The formation of the resonator was confirmed by observing the laser actions of the resonator. Two-dimensional maneuverability was demonstrated by moving the position of lasing spot over the photonic crystal pattern. Spectral tuning was also demonstrated by adjusting the curvature of the microfiber. Efficient extraction is provided by evanescent coupling to the microfiber. These simple but useful functionalities, such as the two-dimensional relocation, spectral tuning, and efficient extraction, which the curved-microfiber coupling offers, are believed to provide an alternative way of coupling with a single QD.

Acknowledgements

This work was supported by Korea Science and Engineering Foundation (KOSEF) (grant code: R31-2008-000-10071-0) grant funded by the Korean government (MEST), the Korea Foundation for International Cooperation of Science and Technology (KICOS) (No. M60605000007-06A0500-00710) through grants provided by the Korean Ministry of Science and Technology (MOST), and the Star-Faculty Project (Grant No. KRF-2007-C00018).

#110883 - $15.00 USD Received 4 May 2009; revised 8 Jul 2009; accepted 8 Jul 2009; published 15 Jul 2009